The Mitochondrial Permeability Transition Is Required for Tumor Necrosis Factor Alpha-Mediated Apoptosis and Cytochrome c Release

CYNTHIA A. BRADHAM,[1] TING QIAN,[3] KONRAD STREETZ,[4] CHRISTIAN TRAUTWEIN,[4]
DAVID A. BRENNER,[1,2]* AND JOHN J. LEMASTERS[3]

Departments of Medicine,[1] Biochemistry & Biophysics,[2] and Cell Biology & Anatomy,[3] University of North Carolina at Chapel Hill, Chapel Hill, North Carolina, and Department of Gastroenterology and Hepatology, Mediziniche Hochschule Hannover, Hannover, Germany[4]

This study assesses the controversial role of the mitochondrial permeability transition (MPT) in apoptosis. In primary rat hepatocytes expressing an IκB superrepressor, tumor necrosis factor alpha (TNFα) induced apoptosis as shown by nuclear morphology, DNA ladder formation, and caspase 3 activation. Confocal microscopy showed that TNFα induced onset of the MPT and mitochondrial depolarization beginning 9 h after TNFα treatment. Initially, depolarization and the MPT occurred in only a subset of mitochondria; however, by 12 h after TNFα treatment, virtually all mitochondria were affected. Cyclosporin A (CsA), an inhibitor of the MPT, blocked TNFα-mediated apoptosis and cytochrome c release. Caspase 3 activation, cytochrome c release, and apoptotic nuclear morphological changes were induced after onset of the MPT and were prevented by CsA. Depolarization and onset of the MPT were blocked in hepatocytes expressing ΔFADD, a dominant negative mutant of Fas-associated protein with death domain (FADD), or crmA, a natural serpin inhibitor of caspases. In contrast, Asp-Glu-Val-Asp-cho, an inhibitor of caspase 3, did not block depolarization or onset of the MPT induced by TNFα, although it inhibited cell death completely. In conclusion, the MPT is an essential component in the signaling pathway for TNFα-induced apoptosis in hepatocytes which is required for both cytochrome c release and cell death and functions downstream of FADD and crmA but upstream of caspase 3.

Apoptosis, or programmed cell death, occurs at all stages of multicellular life and is required during development, immune system function, tissue remodeling, and cancer defense. Apoptotic signaling includes three stages: signal induction, propagation via a protease cascade, and execution. The signal induction stage varies with the stimulus but converges on common propagation and execution stages. The end result of apoptosis is degradation of various cellular proteins, such as nuclear lamins and cytoskeletal components, breakdown of the genomic DNA into internucleosomal fragments, and morphological changes, including cellular shrinking and surface blebbing. Ultimately, the cell and its contents are broken down to membrane-bound fragments that are phagocytosed by adjacent cells (26, 54).

Tumor necrosis factor alpha (TNFα) is a pleiotropic cytokine that can signal for proliferation, stress, inflammation, and cell death (73). TNFα participates in many forms of hepatic pathology, including ischemia/reperfusion injury, alcoholic and viral hepatitis, and injury from hepatotoxins (13, 20, 22, 38). Exogenous TNFα induces fulminant liver failure and hepatocyte apoptosis (38). The p55 TNFα receptor (TNFR-1) forms trimers upon binding to TNFα. The cytoplasmic portion of TNFR-1 then interacts with the adapter protein TNFR-associated death domain protein (TRADD) via a conserved sequence known as the death domain (31). TRADD serves as the branch point for TNFR signaling by binding both TNFR-associated factor 2 (Traf2) and Fas-associated protein with death domain (FADD) (30).

Dominant negative versions of Traf2 block NF-κB activation (43), although Traf2-deficient mice are only mildly impaired in activating NF-κB (76), suggesting that NF-κB activation is signaled through both Traf2-dependent and -independent pathways, possibly involving other Traf family members or RIP (68). NF-κB activation is induced by sequential activation of NIK, which associates with Traf2 (44), and IκB kinase, which phosphorylates IκBα on serines 32 and 36 (18), targeting IκBα for ubiquitination and degradation (9). The loss of IκB binding unmasks the nuclear localization signals on NF-κB, resulting in nuclear relocalization and activation of NF-κB-dependent transcription (5). Resistance to apoptosis is conferred by NF-κB, since inhibition of NF-κB activation renders normally resistant cells sensitive to TNFα- and daunorubicin-mediated cell death (74). This is consistent with previous observations that transcriptional inhibitors enhance the apoptotic response to TNFα (37).

FADD's death effector domain signals apoptosis by binding to caspase 8, the likely candidate for the proximal protease in the caspase cascade (6, 45). Cell death mediated by both TNFα and Fas (a TNFR family member) is blocked in MCF7 cells by stable expression of a FADD mutant which lacks the death effector domain (ΔFADD) and is thus unable to bind caspase 8 (11). In addition, caspase 8 mutants which are non-FADD-interacting (due to truncation) or are catalytically inactive also block Fas- and TNFα-mediated cell death in 293 and HeLa cells (6), further demonstrating the importance of this protein-protein interaction in signaling receptor-mediated apoptosis.

Caspases are a family of cysteine proteases that cleave their substrates after aspartate residues (1, 57). Fas-mediated cell death requires caspase 1, since cells derived from caspase 1-knockout mice resist Fas-mediated apoptosis (36). crmA is a serpin family protease inhibitor produced by cowpox virus that

* Corresponding author. Mailing address: 326 Burnett-Womack C.B. 7080, University of North Carolina at Chapel Hill, Chapel Hill, NC 27599. Phone: (919) 966-0650. Fax: (919) 966-7468. E-mail: dab @med.unc.edu.

blocks TNFα- and Fas-mediated apoptosis (53, 67). Caspases 1 and 8 are inhibited most strongly by crmA, whereas executionary caspases, including caspase 3 (CPP32/YAMA/apopain), are 3 to 4 orders of magnitude less sensitive (79). Activation of caspase 1-like proteases precedes that of caspase 3-like proteases during Fas-mediated apoptosis (19, 64), suggesting that caspase 1-like proteases participate in the receptor-mediated signaling stage, while caspase 3-like proteases are part of the general propagation and/or execution stages of programmed cell death.

Substantial evidence implicates mitochondria in apoptotic signaling. Bcl-2, an antiapoptotic proto-oncogene product, is localized to the mitochondria (17). A series of studies demonstrated that the induction of the mitochondrial permeability transition (MPT) in isolated mitochondria induces apoptotic changes in isolated nuclei (64, 78). Under these conditions, mitochondria release a 50-kDa apoptotic protease, known as apoptosis-inducing factor, which induces the nuclear changes (65). Other studies showed that cytochrome c release from mitochondria is a strong proapoptotic signal and precedes the final execution stage of apoptosis (35, 42, 75).

The MPT represents an abrupt increase of permeability of the inner mitochondrial membrane to solutes with a molecular mass of less than 1,500 Da (see reference 80 for a review). Calcium ions, inorganic phosphate, and oxidant chemicals promote onset of the MPT, whereas cyclosporin A (CsA), an immunosuppressive endecapeptide, specifically blocks onset of the MPT. The rapid increase of permeability associated with the MPT quickly causes depolarization, uncoupling of oxidative phosphorylation, and large-amplitude mitochondrial swelling. Onset of the MPT is caused by the opening of a very large conductance channel or pore in the inner mitochondrial membrane. The molecular composition of the permeability transition pore remains uncertain. The pore may be composed in part of the adenine nucleotide translocator protein in the inner membrane, cyclophilin in the matrix, porin in the outer membrane, and possibly other proteins at contact sites between the inner and outer membranes (80).

Cytochrome c is a 12-kDa protein which functions in the mitochondrial electron transport chain. At physiological ionic strength, cytochrome c diffuses in the aqueous phase between the inner and outer membranes (outer compartment) between complex III (cytochrome bc_1) and complex IV (cytochrome aa_3) (15, 25). After large-amplitude swelling, such as that due to osmotic shock or the MPT, ruptures in the outer membrane permit the release of cytochrome c (72). Thus, onset of the MPT with consequent mitochondrial swelling seems a likely basis for the appearance of cytochrome c in the cytosol during apoptosis. However, two recent studies reported release of cytochrome c during apoptosis that was not accompanied by mitochondrial depolarization (35, 75). Since mitochondrial depolarization invariably follows onset of the MPT, the importance of the MPT in the propagation stage of apoptotic signaling is called into question.

Confocal microscopy can directly visualize onset of the MPT in individual mitochondria of living cells (48). Onset of the MPT is inferred from the redistribution of calcein, a fluorophore of 623 Da, from the cytosol into the mitochondria when mitochondrial membrane permeability increases. The purpose of this study was to characterize the role of the MPT during TNFα-mediated apoptosis using confocal microscopy. The results show that the MPT is induced during apoptosis. In addition, CsA blocks the onset of the MPT, cytochrome c release, and apoptotic cell death, showing that MPT is required for cytochrome c release and apoptosis. We show further that the onset of the MPT lies downstream from FADD and

crmA-inhibitable caspases but upstream of Asp-Glu-Val-Asp (DEVD)-inhibitable caspases.

MATERIALS AND METHODS

Reagents. Reagent-grade chemicals were obtained from Sigma (St. Louis, Mo.) or Fisher Scientific (Pittsburgh, Pa.) unless otherwise noted. Cell culture media were from Gibco BRL Life Technologies (Gaithersburg, Md.). Murine TNFα was from R&D Systems, Inc. (Minneapolis, Minn.), and was used at 30 ng/ml (final concentration). CsA was from Sandoz (Basel, Switzerland). Asp-Glu-aspartic acid aldehyde (DEVD-cho) was from Bachem (King of Prussia, Pa.). Tetramethylrhodamine methylester (TMRM) and calcein-AM were obtained from Molecular Probes (Eugene, Oreg.).

Primary hepatocyte cultures and infections. Primary rat hepatocytes were isolated by collagenase perfusion as described previously (29). Cell viability routinely exceeded 95%. A total of 4×10^6 cells were plated on 100-mm-diameter tissue culture plates coated with 5 mg of rat tail collagen in Waymouth's medium containing 10% fetal calf serum, 0.1 μM insulin, and 0.1 μM dexamethasone. After 2 h, cultures were washed with 1× phosphate-buffered saline and then changed to hormonally defined media (HDM) containing 1 μg of insulin per ml, 5 μg of transferrin per ml, 3 μM selenium, and 10 nM free fatty acids in RPMI basal medium. Cells were infected in HDM with 30 PFU/cell (total of 60 PFU/cell for coinfections) for 2 to 5 h at 37°C and then changed to HDM containing TNFα or other treatments.

Adenoviruses. The adenovirus type 5 (Ad5) variant Ad5IκB, expressing hemagglutinin (HA)-tagged IκBα (S32A, S36A), has been described elsewhere (32). HA-tagged IκB expression was confirmed with Western blotting using an anti-HA monoclonal antibody (Babco, Berkeley, Calif.). The control virus Ad5Luc expresses luciferase driven by a cytomegalovirus promoter (kind gift from Branko Stefanovic). Control adenovirus expression was confirmed by luciferase assays (data not shown). The ΔFADD (NFD-4)- and crmA-expressing viral constructs were prepared by standard molecular biology techniques, using previously described constructs of AU-1-NFD4 (a truncated form of FADD that functions as a dominant negative protein, tagged with an AU-1 epitope) (11) and crmA (67), and the adenoviral transfer vector pACCMV.PLPASR (+), which drives expression with a cytomegalovirus promoter. Adenoviruses were produced by homologous recombination of truncated human Ad5 *dl*309 DNA and transfer vectors in 293 cells, amplified, and purified as described previously (23). crmA and AU-1-ΔFADD expression was verified by Western blotting with anti-crmA polyclonal antiserum (kind gift from M. Tewari and V. M. Dixit) and anti-AU-1 monoclonal antibody (Babco), respectively. Secondary horseradish peroxidase-conjugated antibodies were from Santa Cruz Biotechnology (Santa Cruz, Calif.) and were visualized by enhanced chemiluminescence (Amersham Life Science, Arlington Heights, Ill.). Mobility shift assays for NF-κB DNA binding activity were performed as described previously (7), using a consensus NF-κB binding site probe.

Measurement of apoptosis. For quantitation of cell viability (presented as average ± standard error of the mean [SEM]), cells were infected and treated as described above. After 24 h of TNFα treatment, cells were scored as viable or apoptotic based on morphological criteria and counted. A minimum of 350 cells were counted for each condition. For propidium iodide nuclear staining, 10^6 cells were plated on 60-mm-diameter tissue culture plates coated with 3 mg of rat tail collagen and then infected and treated as described above. Cells were fixed in 3:1 methanol-acetic acid, stained with 10 μg of propidium iodide per ml, and viewed with a Zeiss fluorescence microscope at 400×, using a rhodamine filter set. To assess DNA ladder formation, 4×10^6 cells were digested overnight at 37°C in 0.5 mg of proteinase K per ml–0.5% sarcosyl in 1× phosphate-buffered saline, treated with 10 μg of RNase A for 1 h at 37°C, then gently extracted with phenol and chloroform, and analyzed on 2% agarose gels. Amino-4-trifluoromethyl coumarin (AFC) release assays for caspase 3 activity were performed with a FluorAce kit (Bio-Rad Laboratories, Hercules, Calif.) according to the manufacturer's instructions. Briefly, whole-cell lysates were combined with 25 μM z-DEVD-AFC and incubated for 2 h at room temperature. Change in fluorescence (excitation at 370 nm and emission at 490 nm) was monitored at 1-h intervals, converted to picomoles of AFC released by using a standard curve, and normalized for protein concentration. Assays were performed in duplicate or triplicate.

Cytochrome c measurements. Mitochondrial and S-100 fractions were prepared from 8×10^6 Ad5IκB-infected hepatocytes by differential centrifugation in buffer containing 250 mM sucrose as described previously (75). Protein samples of 25 μg were loaded on sodium dodecyl sulfate–15% polyacrylamide gels, subjected to electrophoresis, and then electrophoretically transferred to nitrocellulose membranes (Schleicher & Schuell, Keene, N.H.). Western blots were probed with primary monoclonal anti-cytochrome c antibody (Pharmingen, San Diego, Calif.) and secondary anti-mouse horseradish peroxidase-conjugated antibody (Santa Cruz Biotechnology) and then developed with enhanced chemiluminescence (Amersham Life Science).

Confocal microscopy. Cell loading and confocal microscopy were carried out essentially as described previously (52). Briefly, 10^6 hepatocytes plated on collagen-coated 40-mm-diameter glass coverslips were infected with adenoviruses and treated as described above in HDM supplemented with 50 mM HEPES (pH 7.0) to stabilize pH during the confocal measurements. After 6 h of treatment
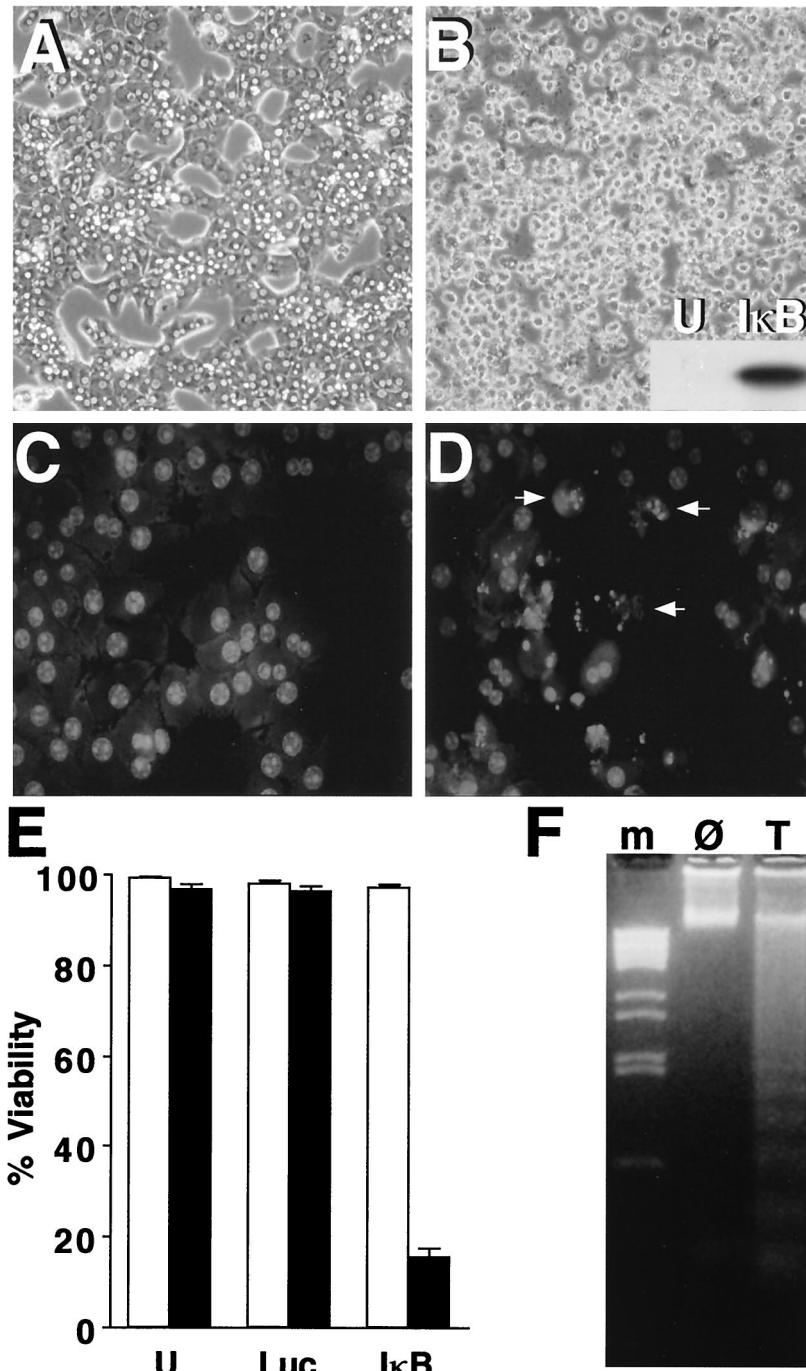
FIG. 1. The IκB superrepressor sensitizes cells to TNFα-mediated apoptosis. Primary hepatocyte cultures were infected with Ad5IκB and then either not treated or treated for 24 h with TNFα (30 ng/ml). (A and B) Phase-contrast photomicrographs showing cellular morphology of untreated (A) and TNFα-treated (B) cells were taken at a magnification of ×100. The inset to panel B shows a Western blot for IκB superrepressor expression in uninfected (U) and Ad5IκB-infected (IκB) hepatocytes. (C and D) Propidium iodide-stained images of untreated (C) and TNFα-treated (D) cells were captured at a magnification of ×400. Arrows indicate representative apoptotic nuclei. (E) Primary hepatocyte cultures were uninfected (U), infected with control virus Ad5Luc (Luc), or infected with Ad5IκB (IκB) and then either not treated (□) or treated for 24 h with 30 ng of TNFα per ml (■). Average percent viability ± SEM is shown. (F) Ad5IκB-infected hepatocytes were either untreated (Ø) or treated with 30 ng of TNFα per ml (T) for 24 h. DNA was then extracted and analyzed for apoptotic ladder formation. Lane m, DNA markers.

with TNFα, cells were loaded with 500 nM TMRM and 1 μM calcein-AM in KRH buffer (29). Subsequently, the TNFα-containing HDM was replaced after supplementation with 100 nM TMRM. Images were collected from 7 to 14 h following TNFα treatment, by using laser scanning confocal microscopy on cells maintained at 37°C. TMRM fluorescence was excited at 568 nm and emission was imaged at >590 nm, by using a long-path emission filter. Calcein fluorescence was excited at 488 nm and emission was collected at 515 to 560 nm, by using a band path emission filter.

RESULTS

Apoptosis model. Hepatocytes resist TNFα-mediated apoptosis unless they are also treated with a protein synthesis inhibitor such as cycloheximide or actinomycin D (37), which probably reflects the protective role of proteins whose expression is stimulated by the transcription factor NF-κB
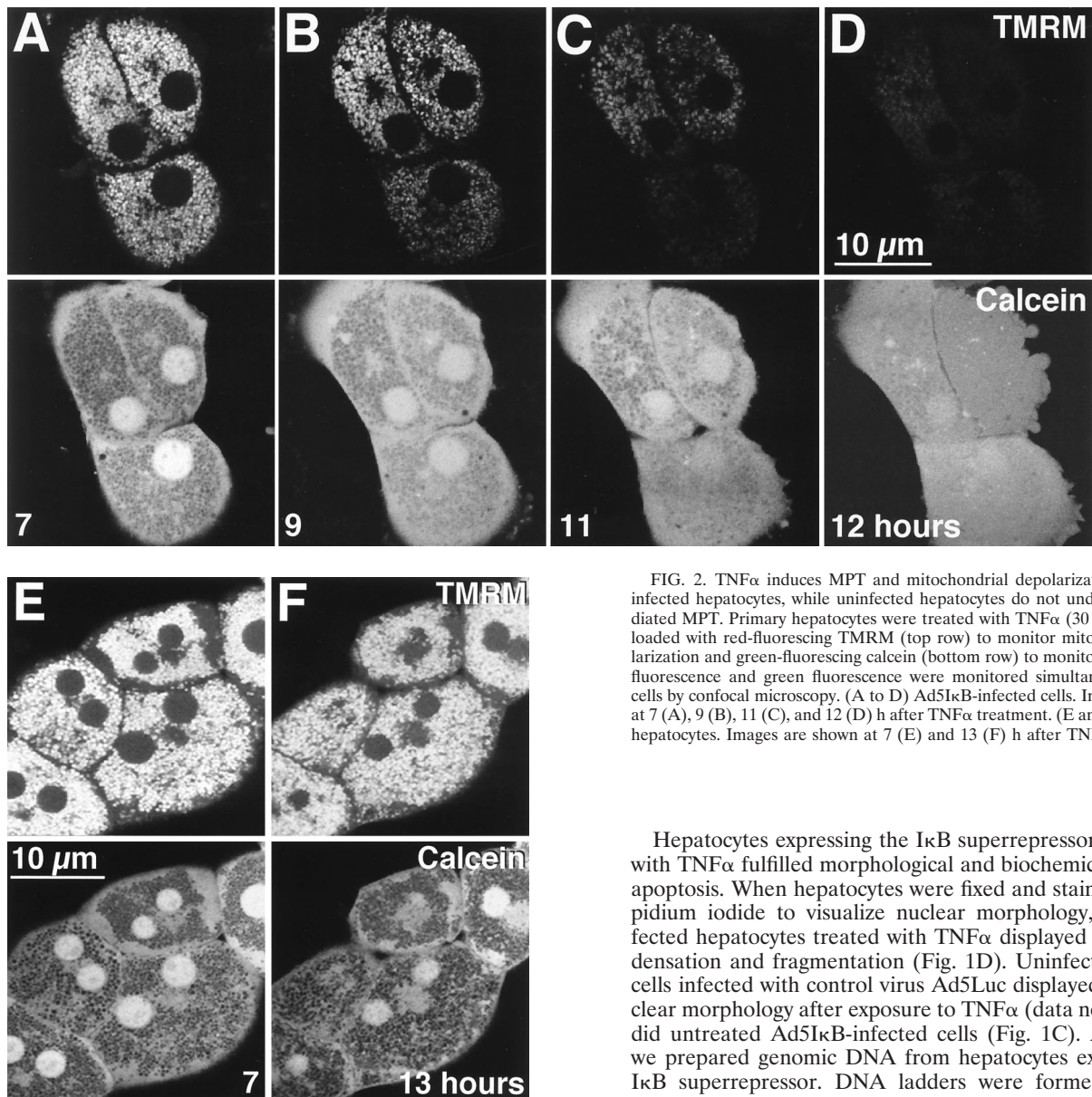
FIG. 2. TNFα induces MPT and mitochondrial depolarization in Ad5IκB-infected hepatocytes, while uninfected hepatocytes do not undergo TNFα-mediated MPT. Primary hepatocytes were treated with TNFα (30 ng/ml) and then loaded with red-fluorescing TMRM (top row) to monitor mitochondrial depolarization and green-fluorescing calcein (bottom row) to monitor the MPT. Red fluorescence and green fluorescence were monitored simultaneously in living cells by confocal microscopy. (A to D) Ad5IκB-infected cells. Images are shown at 7 (A), 9 (B), 11 (C), and 12 (D) h after TNFα treatment. (E and F) Uninfected hepatocytes. Images are shown at 7 (E) and 13 (F) h after TNFα treatment.

(74). To render normally unresponsive hepatocytes sensitive to TNFα-mediated apoptosis, we blocked NF-κB activation by using an IκBα (S34A, S36A)-expressing adenovirus (Ad5IκB) (32). This mutant form of IκBα is not phosphorylated and targeted for degradation and thus prevents NF-κB activation (53). Expression of the HA-tagged IκB superrepressor after Ad5IκB infection was confirmed by Western blotting (Fig. 1B, inset). When primary rat hepatocytes overexpressing the IκB superrepressor were treated with TNFα, the cells lost viability after 24 h, as shown by morphological changes including rounding, loss of attachment, and increased refractility in phase-contrast images (Fig. 1B). Cells expressing the IκB superrepressor but not treated with TNFα did not lose viability (Fig. 1A). Uninfected cells and cells infected with a control adenovirus (Ad5Luc) were not killed after 24 h of TNFα treatment, while Ad5IκB-infected hepatocytes treated with TNFα displayed striking cell death (Fig. 1E).

Hepatocytes expressing the IκB superrepressor and treated with TNFα fulfilled morphological and biochemical criteria of apoptosis. When hepatocytes were fixed and stained with propidium iodide to visualize nuclear morphology, Ad5IκB-infected hepatocytes treated with TNFα displayed nuclear condensation and fragmentation (Fig. 1D). Uninfected cells and cells infected with control virus Ad5Luc displayed normal nuclear morphology after exposure to TNFα (data not shown), as did untreated Ad5IκB-infected cells (Fig. 1C). Additionally, we prepared genomic DNA from hepatocytes expressing the IκB superrepressor. DNA ladders were formed in TNFα-treated but not untreated cells (Fig. 1F). These results show that expression of the IκB superrepressor sensitizes primary hepatocytes to TNFα-mediated apoptosis.

TNFα induces mitochondrial effects during apoptosis. To directly determine the effect of TNFα on mitochondrial function and membrane permeability, we loaded cells with cationic TMRM, a red-fluorescing, membrane potential-indicating fluorophore, and calcein, a green-fluorescing fluorophore that localizes to the cytosol under the loading conditions used (48). After 7 h of treatment with TNFα, the distributions of TMRM (Fig. 2A, top) and calcein (Fig. 2A, bottom) remained normal (for comparison, see reference 39). Each red TMRM-labeled mitochondrion corresponded to a dark void in the green calcein image, showing that the mitochondria were polarized and impermeable to low-molecular-weight solutes. After 9 h of exposure to TNFα, approximately one-third to one-half of the mitochondria lost TMRM fluorescence, indicating depolarization (Fig. 2B, top). Simultaneously, these mitochondria filled with calcein fluorescence, demonstrating permeabilization of the inner mitochondrial membrane to low-molecular-weight solutes, corresponding to onset of the MPT (Fig. 2B, bottom).
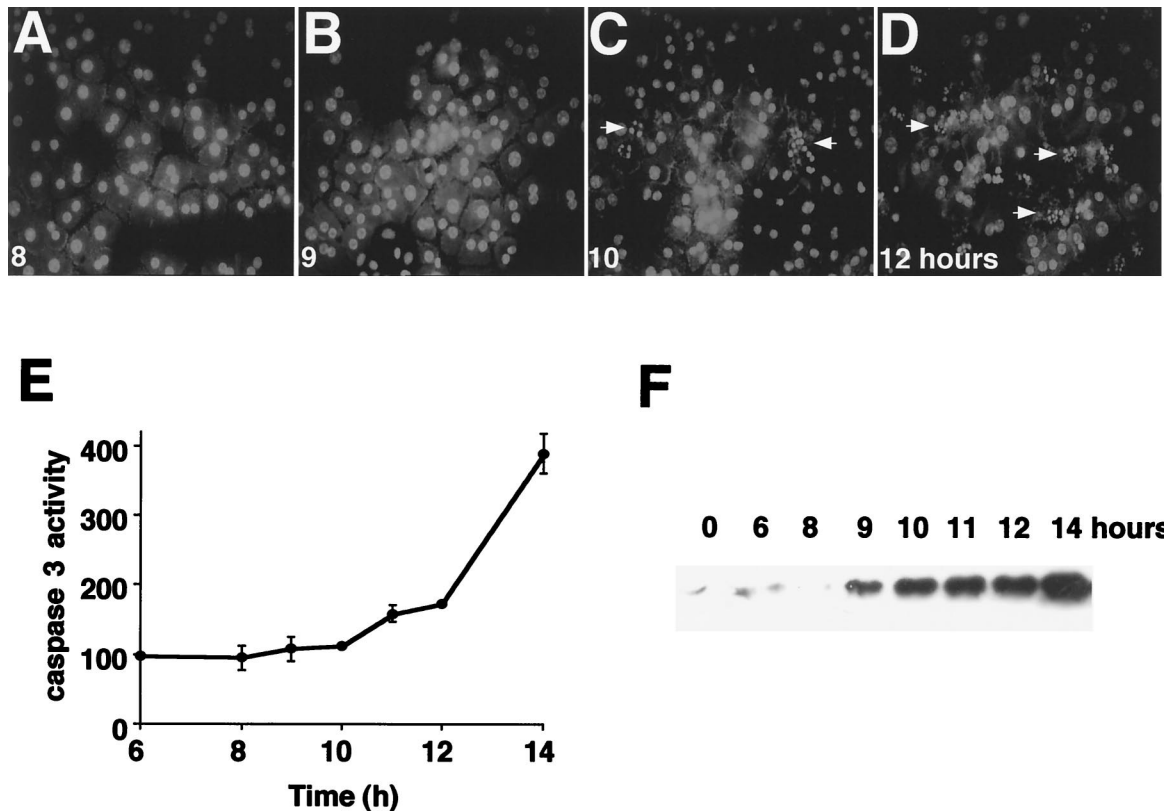
FIG. 3. The MPT precedes nuclear condensation, caspase 3 activation, and cytochrome *c* release. (A to D) Time course of nuclear morphology. Ad5IκB-infected hepatocytes were treated with TNFα (30 ng/ml) and then fixed and stained with propidium iodide at 8 (A), 9 (B), 10 (C), and 12 (D) h after TNFα treatment as for Fig. 1. Arrows indicate apoptotic nuclei. (E) Ad5IκB-infected hepatocytes were treated with TNFα (30 ng/ml) and then lysed and assayed for caspase 3 at 1-h intervals. Data are presented as average picomoles of AFC released per microgram of protein per hour ± SEM. (F) Ad5IκB-infected hepatocytes were treated with TNFα (30 ng/ml); then S-100 fractions were prepared at the indicated time points and analyzed for cytochrome *c* content by Western blotting.

After 11 h of TNFα treatment, more than two-thirds of the mitochondria had undergone these changes (Fig. 2C), and after 12 h, virtually all mitochondria were affected (Fig. 2D). Mitochondria in normal hepatocytes (not expressing the IκB superrepressor) treated with TNFα did not depolarize or undergo MPT, since TMRM and calcein distributions did not change between 7 h (Fig. 2E) and 13 h (Fig. 2F) of treatment. Overall, these results show that the MPT and mitochondrial depolarization occurred in hepatocytes overexpressing the IκB superrepressor in response to TNFα. These mitochondrial changes began in a subset of mitochondria between 7 and 9 h after TNFα treatment and progressed to involve all mitochondria by 13 h of treatment.

Onset of the MPT precedes cytochrome *c* release, nuclear condensation and caspase 3 activation. Hepatocytes overexpressing the IκB superrepressor were treated with TNFα, and the time courses for caspase 3 activation, cytochrome *c* release, and nuclear condensation were determined. Caspase 3 activation was assessed by using DEVD-AFC, the preferred tetrapeptide substrate for caspase 3, conjugated to the fluorophore AFC. Release of the fluorophore is a measure of protease activity. Caspase 3 activation showed a small increase at 11 and 12 h after TNFα treatment, but a substantial increase did not occur until 14 h, well after onset of the MPT (Fig. 3E). Apoptotic changes in nuclear morphology were first observed at 10 h after TNFα treatment and were markedly increased at 12 h of treatment (Fig. 3A to D). Cytochrome *c* release was assessed by Western blotting analysis of S-100 fractions from

IκB-expressing hepatocytes. The results show that cytochrome *c* release was not observed until 9 h after TNFα treatment (Fig. 3F), after onset of the MPT. These results show that onset of the MPT occurs prior to downstream apoptotic events, including nuclear fragmentation, caspase 3 activation, and cytochrome *c* release.

CsA blocks MPT and apoptosis. CsA is a well-established inhibitor of the MPT that functions via a mitochondrial cyclophilin which appears to interact directly with and inhibit the permeability pore (27, 66). This MPT-inhibitory effect of CsA is distinct from its immunosuppressive function, since the MPT is not blocked by FK506, which has immunosuppressive effects similar to those of CsA (24, 28). In addition, the MPT is inhibited by chemical variants of CsA which are not immunosuppressive (47, 61, 70). When hepatocytes overexpressing the IκB superrepressor were treated with TNFα in the presence of 2 μM CsA, mitochondrial depolarization and onset of the MPT were blocked (Fig. 4), since TMRM and calcein distributions did not change between 7 h (Fig. 4A) and 13 h (Fig. 4D) of treatment, confirming the MPT-inhibitory effect of CsA.

To test the ability of CsA to protect against TNFα-mediated apoptosis, we assessed TNFα-induced cell killing of hepatocytes expressing the IκB superrepressor in the presence of 0 to 5 μM CsA. At a concentration of 2 μM or more, CsA prevented cell death (Fig. 5A). This concentration is in keeping with previously reported values, which range from effective CsA concentrations of 0.5 to 5 μM for hepatocyte cultures (51,
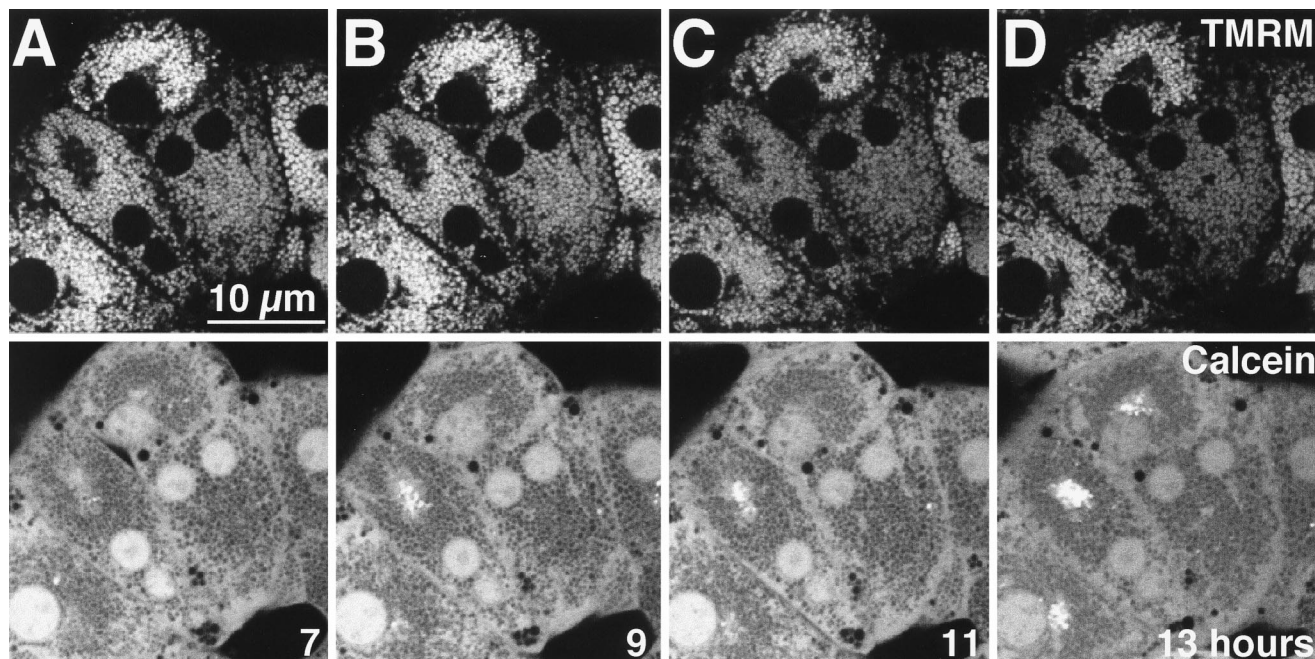
FIG. 4. CsA blocks MPT and depolarization induced by TNFα. Ad5IκB-infected hepatocytes were treated with TNFα (30 ng/ml) and CsA (2 μM), labeled with TMRM (top row) and calcein (bottom row), and analyzed as described for Fig. 2. Images are shown at 7 (A), 9 (B), 11 (C), and 13 (D) h after TNFα-plus-CsA treatment.

52) and 0.1 to 10 μM for purified mitochondria (24, 78). Ethanol vehicle delivered at 1:1,000, corresponding to the highest concentration of CsA used, had no effect on cell viability.

TNFα-mediated cell death became morphologically apparent approximately 16 to 18 h after treatment. Death of all cells was not observed for approximately 24 h. To determine how long after TNFα treatment CsA could be protective, an inhib-

FIG. 5. CsA blocks TNFα-mediated hepatocyte cell death. (A) Dose response of CsA. Ad5IκB-infected hepatocytes were incubated with TNFα (30 ng/ml) and the indicated amounts of CsA for 24 h, and then cell viability was assessed. Average percent viability ± SEM is shown. (B) CsA inhibitor chase experiment. Ad5IκB-infected hepatocytes were treated with TNFα (30 ng/ml) and CsA (2 μM) was added 2 to 16 h later. Cell viability was assessed after 24 h of TNFα treatment. Average percent viability ± SEM is shown.

itor chase experiment was performed. Hepatocytes expressing the IκB superrepressor were first treated with TNFα; at 2-h intervals after TNFα treatment, the cells were exposed to 2 μM CsA. Viability was then assessed after 24 h of TNFα treatment. Cell death was prevented when CsA was added up to 8 h following TNFα but was not blocked when CsA was added 10 or more h after TNFα (Fig. 5B), consistent with time of onset of the MPT.

The MPT is required for caspase 3 activation and cytochrome c release. Caspase 3 was strongly activated in hepatocytes expressing the IκB superrepressor and treated with TNFα (Fig. 6A) but was not active in untreated, IκB-expressing cells (Fig. 6A) or in uninfected or control-infected cells treated with TNFα (data not shown). CsA at 2 μM blocked caspase 3 activation (Fig. 6A), showing that the MPT is required for activation of this downstream protease. Ethanol vehicle (delivered at 1:2,500) had no effect on caspase 3 activity.

To assess the relationship between MPT and cytochrome c release, hepatocytes expressing the IκB superrepressor were either untreated or treated with TNFα with or without CsA. Mitochondrial and S-100 fractions were then prepared after 14 h and analyzed for cytochrome c content by Western blotting. TNFα treatment induced cytochrome c release, as shown by the relative increase in cytochrome c in the S-100 fraction (Fig. 6B, lane 5; Fig. 3F) and decrease in the mitochondrial fraction (Fig. 6B, lane 2) compared to untreated cells (lanes 1 and 4). CsA treatment blocked the release of cytochrome c from the mitochondria to the cytosol (lanes 3 and 6), showing that the MPT is required for cytochrome c release. Ethanol vehicle had no effect on cytochrome c localization.

To rule out the possibility that CsA protected cells by reversing the effect of the IκB superrepressor, we assessed NF-κB activity by using an electrophoretic mobility shift assay with nuclear extracts from uninfected and Ad5IκB-infected hepatocytes treated with 30 ng of TNFα per ml with or without
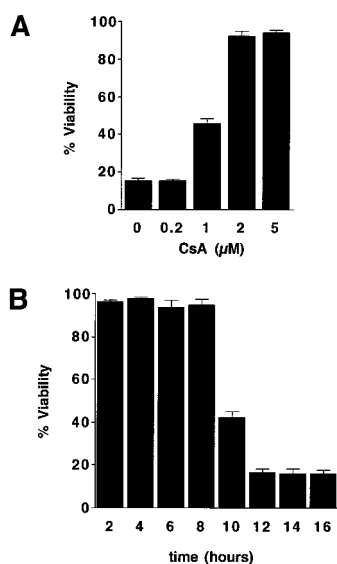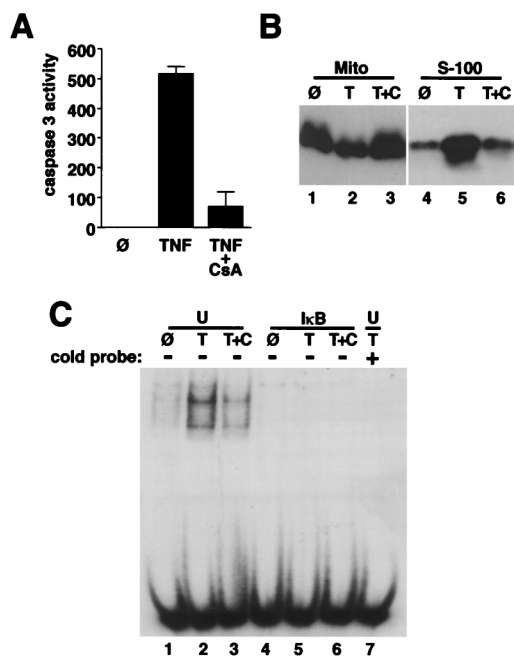
FIG. 6. CsA blocks caspase 3 activation and cytochrome *c* release and does not reactivate NF-κB. (A and B) Ad5IκB-infected hepatocytes were either untreated (Ø) or treated with TNFα (30 ng/ml) alone (T) or with 2 μM CsA (T+C). (A) Caspase 3 activity was assessed after 24 h. Results are presented as average picomoles of AFC released per microgram of protein per hour ± SEM. (B) Mitochondrial (Mito; lanes 1 to 3) and S-100 (lanes 4 to 6) fractions were prepared after 14 h and analyzed for cytochrome *c* content by Western blotting. (C) Uninfected (U) and Ad5IκB-infected (IκB) hepatocytes were either untreated (Ø) or treated with TNFα (30 ng/ml) alone (T) or with 2 μM CsA (T+C) for 30 min. Nuclear extracts were then prepared and analyzed for NF-κB DNA binding activity by using an electrophoretic mobility shift assay. In lane 7, a competition with 200-fold excess unlabeled probe using extract from uninfected, TNFα-treated cells is shown.

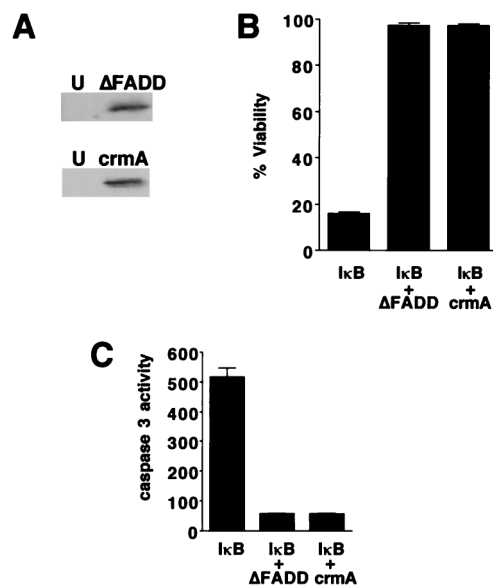FIG. 7. ΔFADD and crmA block TNFα-mediated cell death in Ad5IκB-infected hepatocytes. (A) Western blots showing FADD and crmA expression in uninfected (U) and infected cells. (B and C) Primary hepatocytes were infected with Ad5IκB together with Ad5ΔFADD or Ad5crmA and then treated with TNFα (30 ng/ml). (B) Cell viability was assessed after 24 h of treatment. Average percent viability ± SEM is shown. (C) Caspase 3 activity was assessed after 24 h. Results are presented as average picomoles of AFC released per microgram of protein per hour ± SEM.

2 μM CsA. TNFα treatment for 30 min induced a fourfold increase in NF-κB DNA binding activity in uninfected cells (Fig. 6C, lane 2). Unlabeled oligonucleotide probe at 200-fold excess competed with the labeled probe, demonstrating binding specificity (lane 7). Ethanol vehicle delivered at 1:2,500 had no effect on NF-κB DNA binding activity. CsA partially reduced the increased NF-κB DNA binding activity in response to TNFα in uninfected cells (lane 3), consistent with previous studies (60). In Ad5IκB-infected cells treated with TNFα, NF-κB DNA binding activity was completely blocked as expected (lane 5). CsA did not reverse the complete inhibition of NF-κB DNA binding by the IκB superrepressor (lane 6), confirming that the protection from apoptosis mediated by CsA did not result from reactivating NF-κB. Instead, CsA protected from TNFα-induced apoptosis by an independent mechanism, by blocking the MPT (references 8, 51, 52, 66, 69, and 70 and Fig. 4).

The MPT is downstream from FADD and crmA, and upstream from caspase 3-like proteases. Onset of the MPT precedes caspase 3 activation and apoptotic nuclear alterations, suggesting that the MPT is an upstream component in apoptotic signaling. To address this issue more directly, we used an adenovirus expressing a truncated, dominant negative mutant of FADD (Ad5ΔFADD) to block propagation of apoptotic signals from the TNFR-TRADD complex (11). Expression of ΔFADD in infected cells was confirmed by Western blotting (Fig. 7A). Coexpression of the IκB superrepressor and ΔFADD in hepatocytes resulted in protection from TNFα-

mediated cell death, as expected from previous studies (11) (Fig. 7B). Coexpression of ΔFADD and the IκB superrepressor also prevented caspase 3 activation, nuclear condensation, and DNA ladder formation in response to TNFα (Fig. 7C and data not shown). The onset of the MPT and mitochondrial depolarization were completely blocked in TNFα-treated cells expressing both the IκB superrepressor and ΔFADD (Fig. 8A and B), demonstrating that TNFα-induced onset of the MPT requires FADD.

To assess the role of proximal caspases in signaling to the mitochondria, we used an adenovirus expressing crmA (Ad5crmA), a serpin inhibitor of a subset of caspases, including caspases 1 and 8 (53, 79). crmA expression was confirmed by Western blotting (Fig. 7A). Cells coexpressing the IκB superrepressor and crmA were protected from TNFα-mediated apoptosis, confirming previous findings (67) (Fig. 7B). crmA and IκB superrepressor coexpression in hepatocytes treated with TNFα also inhibited caspase 3 activation, nuclear condensation, and DNA ladder formation (Fig. 7C and data not shown). crmA and IκB superrepressor coexpression blocked both onset of the MPT and the mitochondrial depolarization induced by TNFα (Fig. 8C and D). These results show that the MPT and depolarization lie downstream of the initial induction of crmA-inhibitable caspases.

To further investigate the relationship of the MPT to the apoptotic protease cascade, we treated hepatocytes overexpressing the IκB superrepressor with TNFα in the presence of DEVD-cho, a peptide aldehyde which functions as a competitive inhibitor of caspase 3-subfamily proteases (46). A dose-response study showed that 10 μM was the minimum effective concentration of DEVD-cho that blocked TNFα-mediated cell killing (Fig. 9). In addition, 10 μM DEVD-cho prevented nuclear condensation and DNA ladder formation (data not shown). However, in contrast to the effects of ΔFADD and

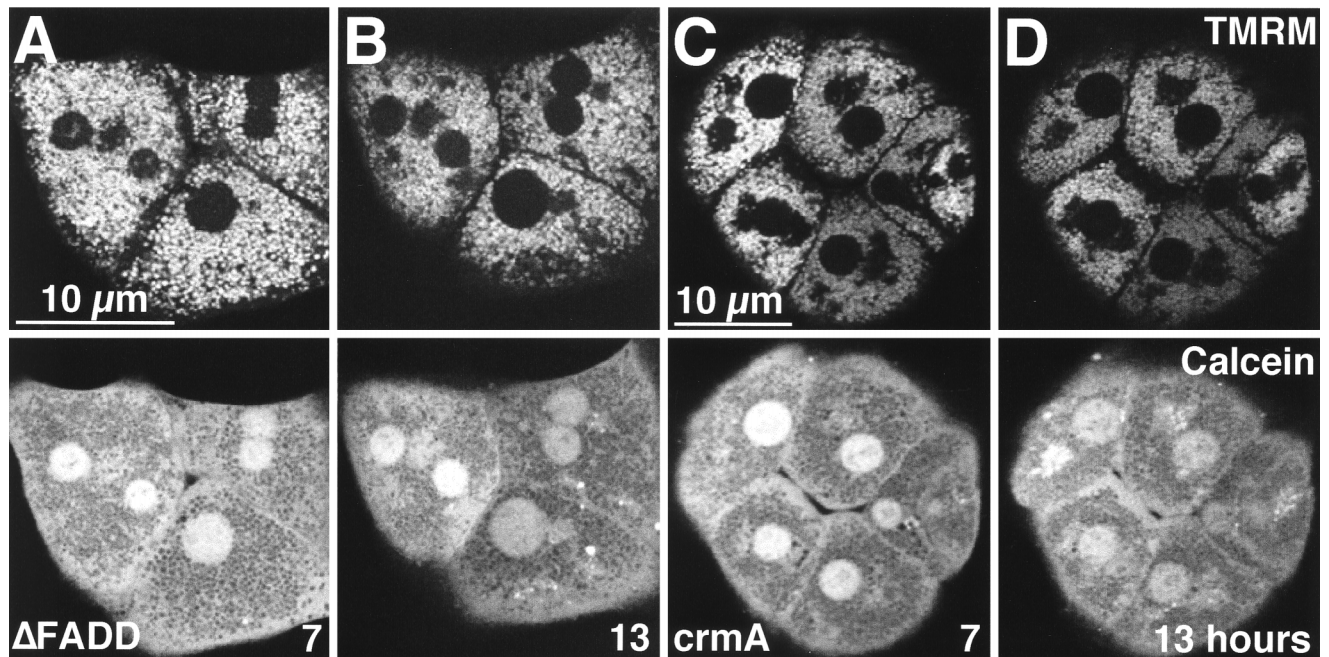FIG. 10. The MPT is upstream from caspase 3. Ad5IκB-infected hepatocytes were treated with TNFα (30 ng/ml) and DEVD-cho (10 μM), labeled with TMRM (top row) and calcein (bottom row), and analyzed as described for Fig. 2. Images are shown at 7 (A), 9 (B), 11 (C), and 13 (D) h after TNFα treatment.

chrome *c* release (Fig. 3) in conjunction with the results of the inhibition experiments (Fig. 6) argue for a model of hepatocyte apoptosis in which the MPT causes cytochrome *c* release. Our results show that the MPT progresses gradually during TNFα-mediated apoptosis, beginning in a subset of mitochondria and requiring several hours to affect all mitochondria (Fig. 2A to D). Thus, for several hours during the apoptotic response, hepatocytes contain both polarized and depolarized mitochondria, the latter being the presumptive source of released cytochrome *c*. This is one possible explanation for the observation that cytochrome *c* is released within cells containing polarized mitochondria. Another possible explanation is suggested by a recent study which defined two distinct pathways for Fas-mediated apoptosis in different cells. In one pathway, both caspase 3 activation and caspase 8 activation occur relatively late, and depend on mitochondrial changes and Bcl-2, while in the other pathway, caspase 8 is activated earlier, and both caspases 3 and 8 are activated independently of the mitochondria and Bcl-2 (58). The discrepancy regarding the role and timing of mitochondrial changes in our system and other systems may reflect a similar duality of signaling pathways induced by TNFα, in parallel to Fas.

Our results show that onset of the MPT precedes nuclear condensation and caspase 3 activation during TNFα-mediated apoptosis (Fig. 3). In addition, we show that the MPT lies downstream of FADD and crmA-inhibitable caspases and upstream of DEVD-sensitive caspases (Fig. 8 and 10). Taken together, these data demonstrate that the MPT is a necessary component of apoptotic signal transduction in primary hepatocytes, functioning as an inte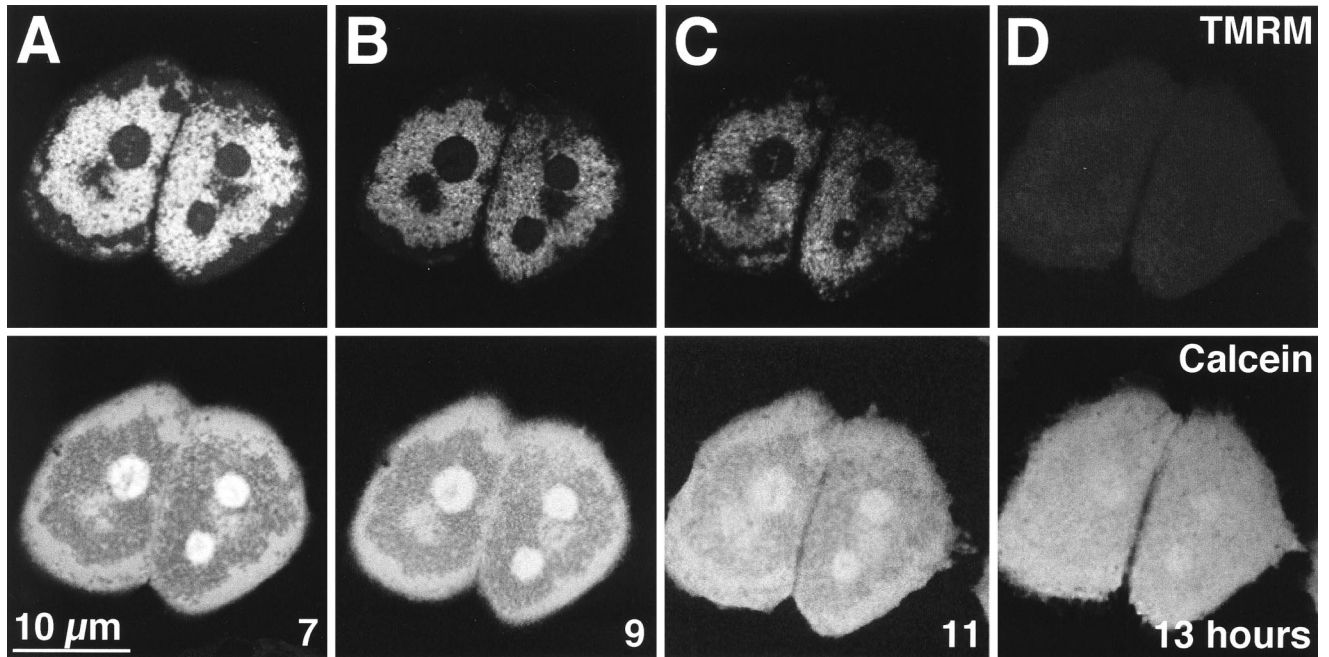rmediate in the caspase cascade. A crmA-sensitive caspase functioning upstream of the mitochondria is in agreement with studies showing that crmA blocks apoptosis induced by TNFR or Fas but does not block killing induced by the proapoptotic mitochondrial protein bax, bik, or bak (10, 49). A caspase induced by TNFα and Fas

upstream from mitochondria may also explain why mitochondrial bcl-2 does not effectively block Fas-mediated cell death (33), since bcl-2 can be converted from anti- to proapoptotic function by caspase-mediated cleavage (10). Our preliminary data indicate that caspase 8 is activated relatively late after TNFα treatment, similar to the type 2 cells described by Scaffidi et al. (58), and not until after onset of the MPT (data not shown). Caspase 1 activity is not induced by TNFα in our system of primary hepatocyte cultures (data not shown). We are currently pursuing studies to identify the upstream caspase or caspases (and their targets) involved in initiating TNFα-mediated MPT and apoptosis.

Cytochrome *c* release is required for caspase 3 activation (41, 81), which is consistent with our results that the MPT lies upstream from caspase 3 activation and is required for cytochrome *c* release in hepatocytes. A likely scenario is that onset of the MPT induces mitochondrial swelling, leading to outer mitochondrial membrane rupture, resulting in cytochrome *c* release. Since bcl-2 inhibits both the MPT and cytochrome *c* release (35, 65, 75, 78), this implies that bcl-2 functions primarily by blocking the MPT, as previously suggested (65). This concept is supported by a recent study showing that bcl-x_L, an antiapoptotic bcl-2 family member, regulates mitochondrial volume homeostasis, preventing the swelling associated with the MPT (71). Another study indicates that bcl-2 maintains mitochondrial polarization by enhancing proton efflux in the presence of uncouplers (63). Further, prevention of cytochrome *c* release is not the only protective function for bcl-x_L, since cells which survive cytochrome *c* microinjection (because they lack caspase 3) undergo TNFα-mediated apoptosis that is inhibited by bcl-x_L (40, 55).

Treatment of isolated mitochondria with the proapoptotic protein bax induces cytochrome *c* release without mitochondrial swelling (34), suggesting that the MPT is not a universal requirement for cytochrome *c* release. However, another study showed that CsA blocks bax-mediated apoptosis and

cytochrome *c* release in Jurkat T cells (50), indicating that bax induces onset of the MPT, which is required for apoptosis, consistent with our results. The mechanism underlying the function of bax is not clear, although there is evidence that bax possesses ion channel-forming activity which is inhibited by bcl-2 (2, 59). Such channels would be too small to directly permit cytochrome *c* release; however, ion flux through such channels could induce opening of the permeability pore, ultimately rupturing the outer mitochondrial membrane.

There is a 9-h delay before the TNFα-induced MPT begins, implying that a checkpoint lies between the TNFR-TRADD-FADD complex and onset of the MPT. Ceramide production is induced in response to TNFα in the pathway between upstream caspases and the mitochondria, since ceramide accumulation is blocked by crmA but not by bcl-2 (16). However, bcl-2 and not crmA blocks ceramide-mediated apoptosis, indicating that ceramides function upstream from mitochondria and the MPT (16). This possibility is further supported by studies showing that cell-permeable C2-ceramide induces mitochondrial effects in hepatocytes (3) and that TNFα treatment of hepatocytes results in a threefold increase in mitochondrial ceramide content (21). Together, these results suggest that the slow accumulation of mitochondrial ceramides may contribute to an apoptotic checkpoint between upstream caspases and onset of the MPT during TNFα-mediated apoptosis.

NF-κB activation blocks MPT induction, since cells not expressing the IκB superrepressor did not undergo depolarization or the MPT in response to TNFα (Fig. 2E and F). This finding indicates that an important protective effect of NF-κB is prevention of the MPT and suggests that NF-κB interferes with the activation of upstream caspases through transcription of a caspase inhibitor similar to crmA. Indeed, NF-κB activates transcription of the caspase inhibitor c-IAP (inhibitor of apoptosis protein), which suppresses apoptosis (12, 77). However, IAPs are unlikely to block the onset of the MPT, since they preferentially bind the distal executionary caspases 3 and 7 and not the proximal caspases (56). In addition, IAPs protect cells from bik- and bak-mediated apoptosis, indicating that they target proteases functioning downstream of the mitochondria (49). Caspase 3 can cleave IκBα in vitro, resulting in a constitutive NF-κB repressor (4), which suggests that distal caspases may in turn inhibit NF-κB to promote apoptosis, as well as potentially feeding back to the mitochondria, further amplifying the MPT. In addition, distal caspases may feed back to amplify proximal caspases. Identification of the NF-κB-inducible gene products that block the upstream pathway will provide new insights into the mechanisms by which TNFα induces either proliferation or apoptosis.

REFERENCES

1. **Alnemri, E. S.** 1997. Mammalian cell death proteases: a family of highly conserved aspartate specific cysteine proteases. J. Cell. Biochem. **64:**33–42.
2. **Antonsson, B., F. Conti, A. Ciavatta, S. Montessuit, S. Lewis, I. Martinou, L. Bernasconi, A. Bernard, J.-J. Mermod, G. Mazzei, K. Maundrell, F. Gambale, R. Sadoul, and J.-C. Matinou.** 1997. Inhibition of Bax channel-forming activity by Bcl-2. Science **277:**370–372.
3. **Arora, A. S., B. J. Jones, T. C. Bronk, and G. J. Gores.** 1997. Ceramide induces hepatocyte cell death through disruption of mitochondrial function in the rat. Hepatology **25:**958–963.
4. **Barkett, M., D. Xue, H. R. Horvitz, and T. D. Gilmore.** 1997. Phosphoryla-

5. tion of IκBα inhibits its cleavage by caspase CPP32 in vitro. J. Biol. Chem. **272:**29419–29422.
5. **Beg, A. A., S. M. Ruben, R. I. Scheinman, S. Haskill, C. A. Rosen, and A. S. J. Baldwin.** 1992. IκB interacts with the nuclear localization sequences of the subunits of NF-κB: a mechanism for cytoplasmic retention. Genes Dev. **6:**1899–1913.
6. **Boldin, M. P., T. M. Goncharov, Y. V. Goltsev, and D. Wallach.** 1996. Involvement of MACH, a novel MORT1/FADD-interacting protease in Fas/APO-1- and TNF receptor-induced cell death. Cell **85:**803–815.
7. **Bradham, C. A., R. Stachlewitz, W. Gao, T. Qian, S. Jayadev, G. Jenkins, Y. Hannun, J. J. Lemasters, R. G. Thurman, and D. A. Brenner.** 1997. Reperfusion after liver transplantation in rats differentially activates the mitogen-activated protein kinases. Hepatology **25:**1128–1135.
8. **Broekmeier, K. M., L. Carpenter-Deyo, D. J. Reed, and D. R. Pfeiffer.** 1992. Cyclosporin A protects hepatocytes subjected to high Ca²⁺ and oxidative stress. FEBS Lett. **304:**192–194.
9. **Brown, K., S. Gerstberger, L. Carlson, G. Franzoso, and U. Siebenlist.** 1995. Control of IκB-α proteolysis by site-specific, signal-induced phosphorylation. Science **267:**1485–1488.
10. **Cheng, E. H.-Y., D. G. Kirsh, R. J. Clem, R. Ravi, M. B. Kastan, A. Bedi, K. Ueno, and J. M. Hardwick.** 1997. Conversion of bcl-2 to a bax-like death effector by caspases. Science **278:**1966–1968.
11. **Chinnaiyan, A. M., C. G. Tepper, M. F. Seldin, K. O'Rourke, F. C. Kischkel, S. Hellbardt, P. H. Krammer, M. E. Peter, and V. M. Dixit.** 1996. FADD/MORT1 is a common mediator of CD95 (Fas/APO-1) and tumor necrosis factor receptor-induced apoptosis. J. Biol. Chem. **271:**4961–4965.
12. **Chu, Z. L., T. A. McKinsey, L. Liu, J. J. Gentry, M. H. Malim, and D. W. Ballard.** 1997. Suppression of tumor necrosis factor-induced cell death by inhibitor of apoptosis c-IAP2 is under NF-κB control. Proc. Natl. Acad. Sci. USA **94:**10057–10062.
13. **Colletti, L. M., D. G. Remick, G. D. Burtch, S. L. Kunkel, R. M. Strieter, and D. A. Campbell.** 1990. Role of tumor necrosis factor-α in the pathophysiological alterations after ischemia/reperfusion injury in the rat. J. Clin. Investig. **85:**1936–1943.
14. **Connern, C. P., and A. P. Halestrap.** 1992. Purification and N-terminal sequencing of peptidyl-prolyl cis-trans-isomerase from rat liver mitochondrial matrix reveals the existence of a distinct mitochondrial cyclophilin. Biochem. J. **284:**381–385.
15. **Cortese, J. D., and C. R. Hackenbrock.** 1993. Motional dynamics of functional cytochrome *c* delivered by low pH fusion into the intermembrane space of intact mitochondria. Biochim. Biophys. Acta **1142:**194–202.
16. **Dbaibo, G. S., D. K. Perry, C. J. Gamard, R. Platt, G. G. Poirier, L. M. Obeid, and Y. A. Hannun.** 1997. Cytokine response modifier A (crmA) inhibits ceramide formation in response to tumor necrosis factor (TNF)-α: crmA and bcl-2 target distinct components in the apoptotic pathway. J. Exp. Med. **185:**481–490.
17. **de Jong, D., F. A. Prins, D. Y. Mason, J. C. Reed, G. B. van Ommen, and P. M. Kluin.** 1994. Subcellular localization of the bcl-2 protein in malignant and normal lymphoid cells. Cancer Res. **54:**256–260.
18. **DiDonato, J. A., M. Hayakawa, D. M. Rothwarf, E. Zandi, and M. Karin.** 1997. A cytokine-responsive IκB kinase that activates the transcription factor NF-κB. Nature **388:**548–554.
19. **Enari, M., R. V. Talanian, W. W. Wong, and S. Nagata.** 1996. Sequential activation of ICE-like and CPP32-like proteases during Fas-mediated apoptosis. Nature **380:**723–726.
20. **Felver, M. E., E. Mezey, M. McGuire, M. C. Mitchell, F. Herlong, G. A. Veech, and R. L. Veech.** 1990. Plasma tumor necrosis factor α predicts decreased long-term survival in severe alcoholic hepatitis. Alcohol Clin. Exp. Res. **14:**255–259.
21. **Garcia-Ruiz, C., A. Colell, M. Mari, A. Morales, and J. C. Fernandez.** 1997. Direct effect of ceramide on the mitochondrial electron transport chain leads to generation of reactive oxygen species. Role of mitochondrial glutathione. J. Biol. Chem. **25:**11369–11377.
22. **Gonzales-Amaro, R., C. Garcia-Monzon, L. Garcia-Buey, R. Moreno-Otero, J. L. Alonso, E. Yague, J. P. Pivel, M. Lopez-Cabrera, E. Fernandez-Ruiz, and F. Sanchez-Madrid.** 1994. Induction of tumor necrosis factor alpha by human hepatocytes in chronic viral hepatitis. J. Exp. Med. **179:**841–848.
23. **Graham, F. L., and L. Prevec.** 1991. Manipulation of adenovirus vectors. Methods Enzymol. **7:**109–128.
24. **Griffiths, E. J., and A. P. Halestrap.** 1991. Further evidence that cyclosporin A protects mitochondria from calcium overload by inhibiting a matrix peptidyl-prolyl cis-trans isomerase. Implications for the immunosuppressive and toxic effects of cyclosporin. Biochem. J. **274:**611–614.
25. **Gupte, S. S., and C. R. Hackenbrock.** 1988. Multidimensional diffusion modes and collision frequencies of cytochrome *c* with its redox partners. J. Biol. Chem. **263:**5241–5247.
26. **Hale, A. J., C. A. Smith, L. C. Sutherland, V. E. A. Stoneman, V. L. Longthorne, A. C. Culhane, and G. T. Williams.** 1996. Apoptosis: molecular regulation of cell death. Eur. J. Biochem. **236:**1–26.
27. **Halestrap, A. P., C. P. Connern, E. J. Griffiths, and P. M. Kerr.** 1997. Cyclosporin A binding to mitochondrial cyclophilin inhibits the permeability

transition pore and protects hearts from ischemia/reperfusion injury. Mol. Cell. Biochem. **174:**167–172.

28. **Henke, W., and K. Jung.** 1993. Comparison of the effects of the immunosuppressive agents FK 506 and cyclosporin A on rat kidney mitochondria. Biochem. Pharmacol. **45:**829–832.

29. **Herman, B., A.-L. Nieminen, G. J. Gores, and J. J. Lemasters.** 1988. Irreversible injury in anoxic hepatocytes precipitated by an abrupt increase in plasma membrane permeability. FASEB J. **2:**146–151.

30. **Hsu, H., H.-B. Shu, M.-G. Pan, and D. V. Goeddel.** 1996. TRADD-TRAF2 and TRADD-FADD interactions define two distinct TNF receptor 1 signal transduction pathways. Cell **84:**299–308.

31. **Hsu, H., J. Xiong, and D. V. Goeddel.** 1995. The TNF receptor 1-associated protein TRADD signals cell death and NF-κB activation. Cell **81:**495–504.

32. **Iimura, Y., T. Nishiura, C. Hellerbrand, K. E. Behrns, R. Schoonhoven, J. W. Grisham, and D. A. Brenner.** 1998. NFκB prevents apoptosis and liver dysfunction during liver regeneration. J. Clin. Investig. **101:**802–811.

33. **Itoh, N., Y. Tsujimoto, and S. Nagata.** 1993. Effect of bcl-2 on Fas antigen-mediated cell death. J. Immunol. **151:**621–627.

34. **Jurgensmeier, J. M., Z. Xie, Q. Devereux, L. Ellerby, D. Bresden, and J. C. Reed.** 1998. Bax directly induces release of cytochrome *c* from isolated mitochondria. Proc. Natl. Acad. Sci. USA **95:**4997–5002.

35. **Kluck, R. M., E. Bossy-Wetzel, D. R. Green, and D. D. Newmeyer.** 1997. The release of cytochrome *c* from mitochondria: a primary site for Bcl-2 regulation of apoptosis. Science **275:**1132–1136.

36. **Kuida, K., J. A. Lippke, G. Ku, M. W. Harding, D. J. Livingston, M. S.-S. Su, and R. A. Flavel.** 1995. Altered cytokine export and apoptosis in mice deficient in interleukin-1β converting enzyme. Science **267:**2000–2003.

37. **Leist, M., F. Gantner, I. Bohlinger, P. G. Germann, G. Tiegs, and A. Wendel.** 1994. Murine hepatocyte apoptosis induced in vitro and in vivo by TNF-alpha requires transcriptional arrest. J. Immunol. **153:**1778–1787.

38. **Leist, M., F. Gantner, H. Naumann, H. Bluethmann, K. Vogt, R. Brigelius-Flohe, P. Nicotera, H.-D. Volk, and A. Wendel.** 1997. Tumor necrosis factor-induced apoptosis during poisoning of mice with hepatotoxins. Gastroenterology **112:**923–934.

39. **Lemasters, J. J., A.-L. Nieminen, T. Qian, L. C. Trost, and B. Herman.** 1997. The mitochondrial permeability transition in toxic, hypoxic and reperfusion injury. Mol. Cell. Biochem. **174:**159–165.

40. **Li, F., A. Srinivasan, Y. Wang, R. C. Armstrong, K. J. Tomaselli, and L. C. Fritz.** 1997. Cell-specific induction of apoptosis by microinjection of cytochrome *c*: bcl-x$_L$ has activity independent of cytochrome *c* release. J. Biol. Chem. **272:**30299–30305.

41. **Li, N. D., I. Budihardjo, S. M. Srinivasula, M. Ahmed, E. S. Alnemri, and X. Wang.** 1997. Cytochrome *c* and dATP-dependent formation of Apaf-1/caspase 9 complex initiates an apoptotic protease cascade. Cell **91:**479–489.

42. **Liu, X., C. N. Kim, J. Yang, R. Jemmerson, and X. Wang.** 1996. Induction of apoptosis in cell-free extracts: requirement for dATP and cytochrome *c*. Cell **86:**147–157.

43. **Liu, Z.-G., H. Hsu, D. V. Goeddel, and M. Karin.** 1996. Dissection of TNF receptor 1 effector functions: JNK activation is not linked to apoptosis while NF-κB activation prevents cell death. Cell **87:**565–576.

44. **Malinin, N. L., M. P. Boldin, A. V. Kovalenko, and D. Wallach.** 1997. MAP3K-related kinase involved in NF-κB induction by TNF, CD-95 and IL-1. Nature **385:**540–544.

45. **Muzio, M., A. M. Chinnaiyan, F. C. Kischkel, K. O'Rourke, A. Shevchenko, J. Ni, C. Scaffidi, J. D. Bretz, M. Zhang, R. Gentz, M. Mann, P. H. Krammer, M. E. Peter, and V. M. Dixit.** 1996. FLICE, a novel FADD-homologous ICE/CED-3-like protease, is recruited to the CD95 (FAS/APO-1) death-inducing signaling complex. Cell **85:**817–827.

46. **Nicholson, D. W., A. Ali, N. A. Thornberry, J. P. Vaillancourt, C. K. Ding, M. Gallant, Y. Gareau, P. R. Griffen, M. Labelle, Y. A. Lazebnik, N. A. Munday, S. M. Raju, M. E. Smulson, T.-T. Yamin, V. L. Yu, and D. K. Miller.** 1995. Identification and inhibition of the ICE/CED-3 protease necessary for mammalian apoptosis. Nature **376:**37–43.

47. **Nicolli, A., E. Basso, V. Petronilli, R. M. Wenger, and P. Bernardi.** 1996. Interactions of cyclophilin with mitochondrial inner membrane and regulation of the permeability transition pore, and cyclosporin A-sensitive channel. J. Biol. Chem. **271:**2185–2192.

48. **Nieminen, A.-L., A. K. Saylor, S. A. Tesfai, B. Herman, and J. J. Lemasters.** 1995. Contribution of the mitochondrial permeability transition to lethal injury after exposure of hepatocytes to *t*-butylhydroperoxide. Biochem. J. **307:**99–106.

49. **Orth, K., and V. M. Dixit.** 1997. Bik and Bak induce apoptosis downstream of crmA but upstream of inhibitor of apoptosis. J. Biol. Chem. **272:**8841–8844.

50. **Pastorino, J. G., S. T. Chen, M. Tafani, and J. L. Farber.** 1998. The over-expression of Bax produces cell death upon induction of the mitochondrial permeability transition. J. Biol. Chem. **273:**7770–7775.

51. **Pastorino, J. G., J. W. Snyder, A. Serroni, J. B. Hoek, and J. L. Farber.** 1993. Cyclosporin and carnitine prevent the anoxic death of cultured hepatocytes by inhibiting the mitochondrial permeability transition. J. Biol. Chem. **268:**13791–13798.

52. **Qian, T., A.-L. Nieminen, B. Herman, and J. J. Lemasters.** 1997. Mitochon-

drial permeability transition in pH-dependent reperfusion injury to rat hepatocytes. Am. J. Physiol. **273:**C1783–C1792.

53. **Ray, C. A., R. A. Black, S. R. Kronheim, T. A. Greenstreet, P. R. Sleath, G. S. Galvesen, and D. J. Pickup.** 1992. Viral inhibition of inflammation: cowpox virus encodes an inhibitor of the interleukin-1β converting enzyme. Cell **69:**597–604.

54. **Rosen, A., and L. Casciola-Rosen.** 1997. Macromolecular substrates for the ICE-like proteases during apoptosis. J. Cell. Biochem. **64:**50–54.

55. **Rosse, T., R. Olivier, L. Monney, M. Rager, S. Conus, I. Fellay, B. Jansen, and C. Borner.** 1998. Bcl-2 prolongs cell survival after bax-induced release of cytochrome *c*. Nature **391:**496–499.

56. **Roy, N., Q. L. Deveraux, R. Takahashi, G. S. Salveson, and J. C. Reed.** 1997. The c-IAP-1 and c-IAP-2 proteins are direct inhibitors of specific caspases. EMBO J. **16:**6914–6925.

57. **Salveson, G. S., and V. M. Dixit.** 1997. Caspases: intracellular signaling by proteolysis. Cell **91:**443–446.

58. **Scaffidi, C., S. Fulda, A. Srinivasan, C. Fiesen, F. Li, K. J. Tomaselli, and M. E. Peter.** 1998. Two CD95 (APO-1/Fas) signaling pathways. EMBO J. **17:**1675–1687.

59. **Schlesinger, P. H., A. Gross, X.-M. Yin, K. Yamamoto, M. Saito, G. Waksman, and S. J. Korsmeyer.** 1997. Comparison of the ion channel characteristics of proapoptotic BAX and antiapoptotic BCL-2. Proc. Natl. Acad. Sci. USA **94:**11357–11362.

60. **Schmidt, A., L. Henninghausen, and U. Siebenlist.** 1990. Inducible nuclear factor binding to the kappa B elements of the human immunodeficiency virus enhancer in T cells can be blocked by cyclosporin A in a signal-dependent manner. J. Virol. **64:**4037–4041.

61. **Schweizer, M., J. Schengel, D. Baumgartner, and C. Richer.** 1993. Sensitivity of mitochondrial peptidyl-prolyl cis-trans isomerase, pyridine nucleotide hydrolysis and Ca^{2+} release to cyclosporin A and related compounds. Biochem. Pharmacol. **45:**641–646.

62. **Shi, Y. F., B. M. Sahai, and D. R. Green.** 1989. Cyclosporin A inhibits activation-induced cell death in T-cell hybridomas and thymocytes. Nature **339:**625–626.

63. **Shimizi, S., Y. Eguchi, W. Kamiike, Y. Funahashi, A. Mignon, V. Lacronique, H. Matsuda, and Y. Tsujimoto.** 1998. Bcl-2 prevents apoptotic mitochondrial dysfunction by regulating proton flux. Proc. Natl. Acad. Sci. USA **95:**1455–1459.

64. **Susin, S. A., N. Zamzami, M. Castedo, E. Daugas, H.-G. Wang, S. Geley, F. Fassy, J. C. Reed, and G. Kroemer.** 1997. The central executioner of apoptosis: multiple connections between protease activation and mitochondria in Fas/APO-1/CD95- and ceramide-induced apoptosis. J. Exp. Med. **186:**25–37.

65. **Susin, S. A., N. Zamzami, M. Castedo, T. Hirsch, P. Marchetti, A. Macho, E. Daugas, M. Geuskens, and G. Kroemer.** 1996. Bcl-2 inhibits the mitochondrial release of an apoptogenic protease. J. Exp. Med. **184:**1331–1341.

66. **Szabo, I., and M. Zoratti.** 1991. The giant channel of the inner mitochondrial membrane is inhibited by cyclosporin A. J. Biol. Chem. **266:**3376–3379.

67. **Tewari, M., and V. M. Dixit.** 1995. Fas- and tumor necrosis factor-induced apoptosis is inhibited by poxvirus *crmA* gene product. J. Biol. Chem. **270:**3255–3260.

68. **Ting, A. T., F. X. Pimentel-Muinos, and B. Seed.** 1996. RIP mediates tumor necrosis factor receptor 1 activation of NF-kappaB but not Fas/APO-1-initiated apoptosis. EMBO J. **15:**6189–6196.

69. **Trost, L. C., and J. J. Lemasters.** 1996. The mitochondrial permeability transition: a new pathophysiological mechanism for Reye's syndrome and toxic liver injury. J. Pharmacol. Exp. Ther. **278:**1000–1005.

70. **Trost, L. C., and J. J. Lemasters.** 1997. Role of the mitochondrial permeability transition in salicylate toxicity to cultured rat hepatocytes: implications for the pathogenesis of Reye's syndrome. Toxicol. Appl. Pharmacol. **147:**431–441.

71. **Vander Heiden, M. G., N. S. Chandel, E. K. Williamson, P. T. Schumacker, and C. B. Thompson.** 1997. Bcl-x$_L$ regulates the membrane potential and volume homeostasis of mitochondria. Cell **91:**627–637.

72. **Vanderkooi, J., M. Erecinska, and B. Chance.** 1973. Cytochrome *c* interaction with membranes. I. Use of a fluorescent chromophore in the study of cytochrome *c* interaction with artificial membranes. Arch. Biochem. Biophys. **154:**219–229.

73. **Wallach, D., M. Boldin, E. Varfolomeev, R. Beyaert, P. Vandenabeele, and W. Fiers.** 1997. Cell death induction by receptors of the TNF family: towards a molecular understanding. FEBS Lett. **410:**96–106.

74. **Wang, C.-Y., M. W. Mayo, and A. S. J. Baldwin.** 1996. TNF- and cancer therapy-induced apoptosis: potentiation by inhibiting NF-κB. Science **274:**784–787.

75. **Yang, J., X. Liu, K. Bhalla, C. N. Kim, A. M. Ibrado, J. Cai, T.-I. Peng, D. P. Jones, and X. Wang.** 1997. Prevention of apoptosis by bcl-2: release of cytochrome *c* from mitochondria blocked. Science **275:**1129–1132.

76. **Yeh, W. C., A. Shaninian, D. Speiser, J. Kraunus, F. Billia, A. Wakeham, J. L. de la Pompa, D. Ferrick, B. Hum, N. Iscove, P. Ohashi, M. Rothe, D. V. Goeddel, and T. M. Mak.** 1997. Early lethality, functional NF-κB activation, and increased sensitivity to TNF-induced cell death in TRAF2-deficient mice. Immunity **7:**715–725.

77. **You, M., P. T. Ku, R. Hrdlickova, and H. R. J. Bose.** 1997. ch-IAP, a member of the inhibitor-of-apoptosis protein family, is a mediator of the antiapoptotic activities of the v-Rel oncoprotein. Mol. Cell. Biol. **17:**7328–7341.
78. **Zamzami, N., S. A. Susin, P. Marchetti, T. Hirsch, I. Gomez-Monterrey, M. Castedo, and G. Kroemer.** 1996. Mitochondrial control of nuclear apoptosis. J. Exp. Med. **183:**1533–1544.
79. **Zhou, Q., S. Snipas, K. Orth, M. Muzio, V. M. Dixit, and G. S. Salveson.** 1997. Target protease specificity of the viral serpin crmA: analysis of five caspases. J. Biol. Chem. **272:**7797–7800.
80. **Zoratti, M., and I. Szabo.** 1995. The mitochondrial permeability transition. Biochim. Biophys. Acta **1241:**139–176.
81. **Zou, H., W. J. Henzel, X. Liu, A. Lutschg, and X. Wang.** 1997. Apaf-1, a human protein homologous to C. elegans CED-4, participates in cytochrome *c*-dependent activation of caspase-3. Cell **90:**405–413.